Automatic Cell Classification in Human's Peripheral Blood Images Based on Morphological Image Processing

Kyungsu Kim[1], Jeonghee Jeon[1], WanKyoo Choi[2], Pankoo Kim[3], Yo-Sung Ho[1]

[1] Kwangju Institute of Science and Technology (K-JIST), 1 Oryong-dong Puk-gu, Kwangju, 500-712, Korea,
{arieskim, jhjeon, hoyo}@kjist.ac.kr,
[2] Division of Computer, Electronics & Communiation Engineering, Kwangju University, 591-1 Jinwol-dong Nam-gu, Kwangju, 503-703, Korea,
wkchoi@kwangju.ac.kr
[3] College of Electronics and Information Engineering, Chosun University, Kwangju, 501-759, Korea,
pkkim@chosun.ac.kr

Abstract. A new scheme for automatic analysis and classification of cells in peripheral blood images is presented in this paper. The proposed method can analyze and classify mature red-blood and white-blood cells efficiently. After we identify red-blood and white-blood cells in a blood image captured by a CCD camera attached to a microscope, we extract their features and classify them by a neural network model based on back-propagation learning. While we have fifteen different clusters including the normal one for red-blood cells, there are five different categories for white-blood cells. We also propose a new segmentation algorithm to extract the nucleus and cytoplasm for white-blood cell classification. In addition, we apply the principal component analysis to reduce the dimension of feature vectors efficiently without affecting classification performance. Experimental results demonstrate that the proposed method outperforms the learning vector quantization-3 and the k-nearest neighbor algorithms for blood cell classification.

1 Introduction

Various algorithms for automated analysis and recognition of medical images have been proposed in conjunction with advanced artificial intelligence, image processing, and computer graphics techniques [1], [4], [9], [13]. As consequences, several automatic medical diagnosis systems have been developed to help doctors to diagnose diseases. Especially, red-blood and white-blood cells of human beings provide valuable information to pathologists. Such information is used to diagnose patients' diseases and allows pathologists to identify morphological variations of blood cells. However, the inspection is time-consuming and requires technical knowledge. With computer-aided inspection systems, pathologists can have objective analysis results of blood cell images and the false inspection ratio

can be reduced significantly. If some part of the inspection job is automated, a technician can save his or her time and effort substantially. Recently, there was an attempt to differentiate the normal white-blood cell from three kinds of leukemia cells. However, it is a very difficult task even for a specialist [1].

Generally, we can observe red-blood cells, white-blood cells, platelets, and plasmas in the image of the human peripheral blood sample by the microscope. Based on the shape and color of the nucleus and cytoplasm, we can classify white-blood cells into five different types: neutrophil, eosinophil, basophil, lymphocyte, and monocyte, as shown in Figure 1.

Fig. 1. Mature white-blood cells.

In this paper, we focus on building a practical system that can be used in the hospital. We classify fifteen different types of red-blood cells including the normal one, as shown in Figure 2, referencing hematology literatures and using pathologist's aids [5].

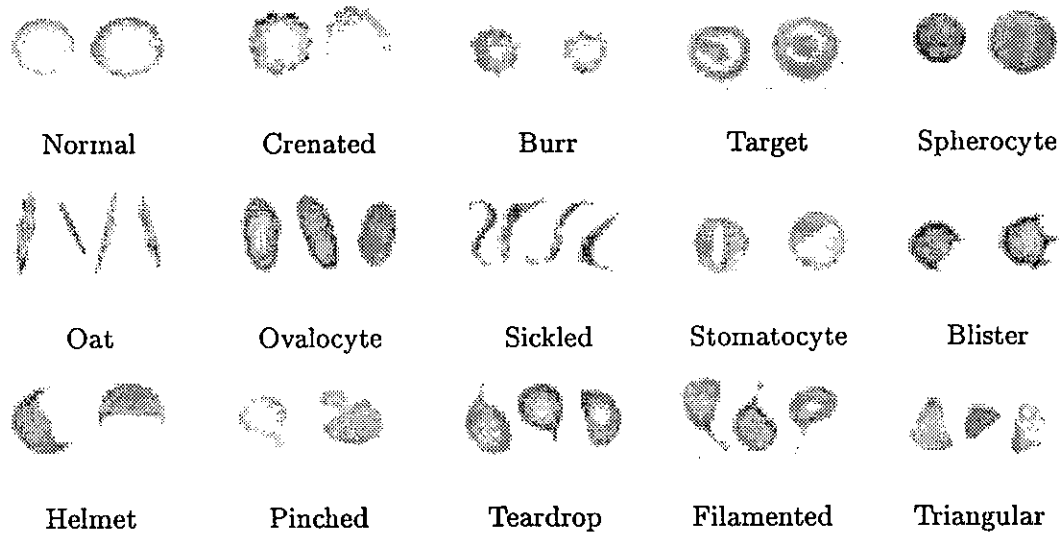

Fig. 2. Morphological shapes of red-blood cells

In the proposed system, we classify and count red-blood and white-blood cells automatically. In our experiment, we design a cell classifier using a neural

network model and compare its performance with two other classifiers: learning vector quantization-3 (LVQ-3) and k-nearest neighbor (K-NN) algorithms. We also reduce the number of multi-variate features using the principal component analysis (PCA) to construct a more efficient classifier.

This paper is organized as followings. Section 2 describes preprocessing, feature extraction and classification algorithms for blood cell analysis. After we present experimental results in Section 3, we draw conclusions in Section 4.

2 Classification of Blood Cells

2.1 Preprocessing

Input images are captured from the color CCD camera attached to a microscope, magnified four hundred times with the resolution of 640x480 pixels. Figure 3(a) shows an input image. Since the clinical pathologist generally examines the ideal zone that has quite a few folded cells, we select the image that is noise free and well focused.

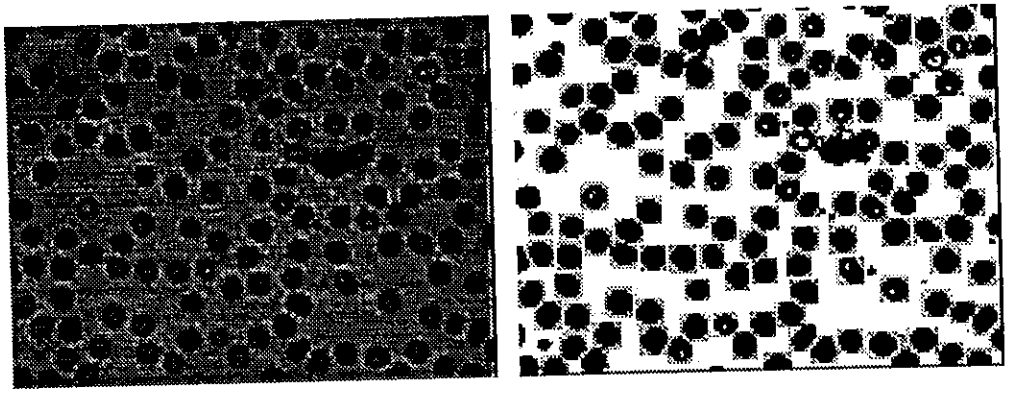

(a) Input image (b)Labeled image

Fig. 3. Preprocessing of the input image.

For the input image, we apply a luminance thresholding method using a fuzzy measure [3] to separate red-blood and white-blood cells from the background of the image. In the labeling step, we exclude boundary cells of the target image. Each labeled cell is classified into one of red-blood cells, white-blood cells, platelets and plasmas based on its size and color. While the white-blood cell has the biggest size and has a nucleus in it, the plasma and the platelet are considerably smaller compared to red-blood and white-blood cells, as demonstrated in Figure 3(a). Figure 3(b) displays labeled cells enclosed by the minimum bounding rectangular boxes.

2.2 Segmentation

In order to separate the white-blood cell into the nucleus and cytoplasm, we propose a hybrid segmentation scheme based on regions and edges. After we enhance image edges and remove noises by the nonlinear anisotropic diffusion algorithm [10], we apply a watershed transform to the image [6], [8]. We then merge the nearest regions by the k-means algorithm based on color information.

Once we apply PCA and the nonlinear anisotropic diffusion algorithm to the input image, we can obtain important edge information by fusing the first component and other two components with appropriate weighting factors. Comparing to other noise filtering methods, the nonlinear diffusion algorithm has good characteristics of removing noises while preserving the edge information. Since the proposed segmentation method employs the watershed transform, PCA and the nonlinear diffusion algorithms are very effective. PCA, also known as the Karhunen-Loeve decomposition, can be used to find eigenvectors of the covariance matrix. In this paper, we employ the linear PCA and use the covariance matrix of each RGB color component to obtain eigenvectors and eigenvalues.

After the PCA operation, a fused image A_n is generated. Regardless of the color model adopted, we can assume that e_1, e_2, and e_3 are the eigenvalues of three principal components of the color. Weighting factors for those color components are calculated by

$$\alpha_1 = \frac{e_1}{e_1 + e_2 + e_3},\ \alpha_2 = \frac{e_2}{e_1 + e_2 + e_3},\ \alpha_3 = \frac{e_3}{e_1 + e_2 + e_3}. \tag{1}$$

In this paper, we employ a nonlinear anisotropic diffusion algorithm [10] to avoid image blurring and solve the local problem of the linear diffusion filtering operation. The nonlinear diffusion operation can be expressed in terms of the time variable t as

$$\frac{\partial I(x,y,t)}{\partial t} = c(x,y,t)\Delta I(x,y,t) + \nabla c(x,y,t)\nabla I(x,y,t) \tag{2}$$

where Δ and ∇ are the Laplacian and the gradient operators, respectively, I(x,y,t) represents the image at time t, and c(x, y, t) is the diffusion conductance coefficient and is globally changed by the local edge analysis. Perona and Malik proposed a function for the intensity gradient [10] as

$$g(\nabla I) = \frac{1}{1 + (\|\nabla I\|/K)^2} \text{ or } g(\nabla I) = exp\left(-\left(\frac{|\nabla f|}{K}\right)^2\right) \tag{3}$$

where K is a conductance variable that controls the gradient of the image. Ideally, K should be selected to reflect the gradient over the whole image or neighboring gradient values of each pixel. The time variable t controls the quantity of diffusion and it plays as the scale variable of the Gaussian blurring operation. If we set a larger value for t, the image will get more diffused. The nonlinear anisotropic diffusion algorithm has advantages in two aspects. It can reduce noises effectively while preserving the edge information, compared to other noise

filtering algorithms: median filtering and Gaussian filtering. The popular watershed algorithm may result in oversegmention, if noises in the input image are not properly removed. However, we do not have the oversegmentation problem with the nonlinear anisotropic diffusion algorithm.

In general, an edge-based segmentation algorithm needs a robust edge linking operation due to edge discontinuity. However, the watershed transform does not need any edge linking opeation, since regions are defined by closed curves. The watershed transform can be implemented by rain falling or hill climbing operation. In this paper, we employ the rain-falling method that consists of the following two steps. Firstly, we define a threshold value. If one pixel has a smaller value than its neighboring pixels, it is considered to belong to the same region. In the next step, remaining pixels are merged to neighboring pixels that have the biggest slope. It is analogous that water in the surface of topology flows to the direction of lower slope.

In order to prevent oversegmenation by the watershed transform, we need to apply a postprocessing algorithm over segmented regions. In this paper, we employ the k-means algorithm, and the average intensity value of each segmented region is used as the measure for merging.

We compare the proposed method with the nonparametric clustering algorithm that was originally proposed for leukemia diagnosis [1]. As shown in Figure 4(a), the nonparametirc algorithm does not segment the input image properly into the nucleus and cytoplasm. Although the region merging algorithm affects the result, the proposed method segments regions intuitively. Figure 4(a) and Figure 4(b) demonstrate the segmentation results of white-blood cells by the nonparametric clustering method and the proposed method, respectively. Figure 5 shows another segemntation result by the proposed method.

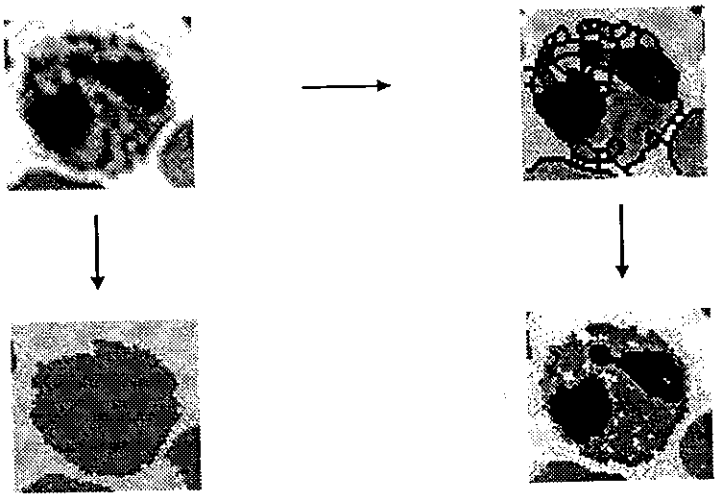

(a) Nonparametric method (b) Proposed method

Fig. 4. Comparison of segmentation results

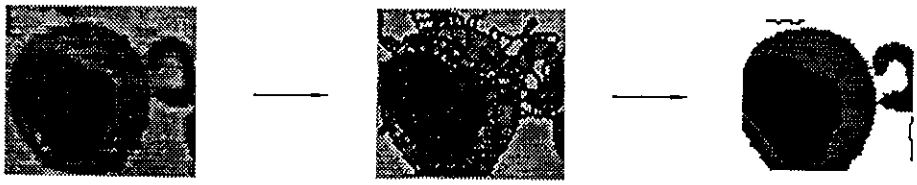

Fig. 5. Segmentation of white-blood cells

2.3 Feature Extraction

Once we label red-blood cells in the input image, we extract image features from each red-blood cell. The red-blood cells are then classified in two steps. Features extracted in the first step are different from those extracted in the second step. We assume that they belong to the same class.

In the first step, since normal, spherocyte, target and stomatocyte cells have the circular shape, the contour information of each cell is used for classification. In the second step, we use all edge information including interior edges as well as their contour information. In order to extract image features, we employ the Universidade Nova de Lisboa (UNL) Fourier transform [11] that is an improved extension of the Fourier descriptor to handle open curves and lines.

We obtain image features as follows. The input image consisting of binary curve patterns is transformed from the Cartesian coordinate system to the polar coordinate system by the UNL transform. After an analytic curve equation is estimated, the transformed curve is instantiated in the polar coordinate system.

Let $\Omega(t)$ be a discrete object composed of n pixels $z_i = (x_i, y_i)$, $O = (O_x, O_y)$ be the centroid of the object, and M be the maximum Euclidean distance from the centroid Ω to all pixels z_i. A discrete object $U(\Omega(t))$ consists of $(U(z_{ij}(t))$, a set of line segments $z_{ij}(t)$ between two neighboring pixels $z_i = (x_i, y_i)$ and $z_j = (x_j, y_j)$.

The UNL transform of the discrete object is defined by the mapping from the Cartesian to the polar coordinate systems.

$$(U(z_{ij}(t)) = \xi_{ij} = (E_{ij}(t), \Theta_{ij}(t)) = \left(\frac{\|z_i + t(z_j - z_i) - O\|}{M},\ arctan\left(\frac{y_i + t(y_j - y_i) - O_y}{x_i + t(x_j - x_i) - O_x}\right)\right) \tag{4}$$

Let $i(x, y)$ be a two-dimensional image that represents a discrete object $\Omega(t)$ and $f(R, \theta)$ be the two dimensional image that represents the UNL transform of $\Omega(t)$. The discrete UNL Fourier features of the object $\Omega(t)$ are the normalized discrete Fourier spectrum $UFF(u', v') = \frac{\|F\{f(R,\theta)\}\|}{F(0,0)} = \frac{\|F(U,v)\|}{F(0,0)}$ of the image $f(R, \theta)$, ignoring $F(0, 0)$ and the values that are duplicated by conjugate symmetry. In this paper, the dimension of extracted features is 76. Figure 6 shows the process to extract edge information of red-blood cells as a preprocessing step for feature extraction.

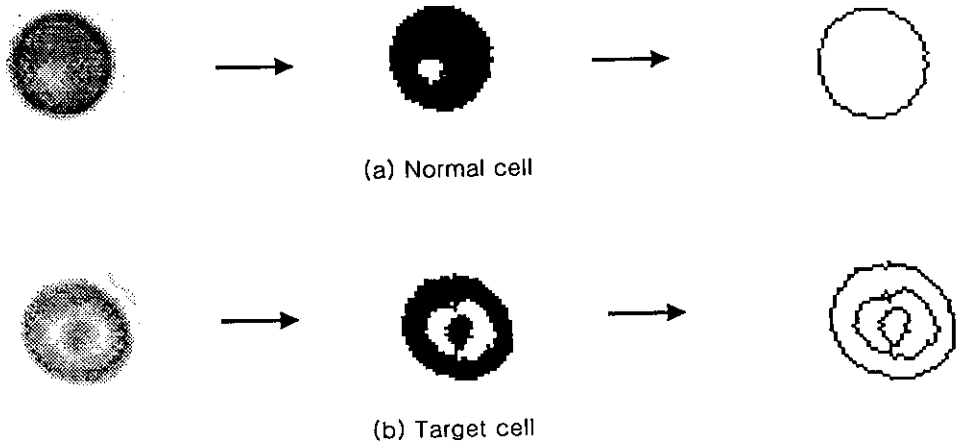

Fig. 6. Feature extraction process of red-blood cells

We have also tested various features of white-blood cells. We categorize the set of features into three groups. Basic features, such as color, size, intensity, ratio of the nucleus and cytoplasm, are included in first category. Second group features are circularity, eccentricity, elongatedness, convexity, and invariant moment features for the shape of the nucleus. Texture features of the nucleus and cytoplasm are included in the third category, where we choose the best 60 features among them.

In order to construct the classifier efficiently, we can extract image features by filtering and wrapping[11]. In this paper, we use the principal component analysis (PCA), one of the popular filtering methods, to extract lower dimensional features by analyzing multi-dimensional features statistically [12]. For red-blood cells, we reduce the extracted 76 dimensional features to 38 dimensional features in the first recognition step by applying PCA. In the second step, we can reduce the initial 76 dimensional features to 67 dimensional features. For white-blood cells, we reduce the 60 dimensional features to 52 dimensional features. Finally, each feature value is normalized to a number between 0 and 1.

2.4 Classification

In this chapter, we introduce a neural network classifier based on the back-propagation learning algorithm and compare the performance of the classification model with the k-nearest neighbor (K-NN) and the learning vector quantization-3 (LVQ-3) algorithms. While K-NN is one of the statistical pattern classification methods, LVQ-3 is one of the clustering algorithms.

Our classifier is a hierarchical neural network model to classify red-blood and white-blood cells using the back-propagation learning algorithm [2]. Classification of red-blood cells consists of two steps. We assume that normal, target, spherocyte and stomatocyte cells of circular contour are included in the same class in the first step. Therefore, each input cell is classified into one of 12 classes.

If a cell has a circular contour, it is classified into one of 4 classes in the second step. The classifier for white-blood cells has the same architecture as the one for red-blood cells, but it has different parameters.

Figure 7 shows a classifier consisting of two neural networks connected in cascade. Another neural network can be added to classify white-blood cells. Table 1 lists parameter values for the three neural networks (NN).

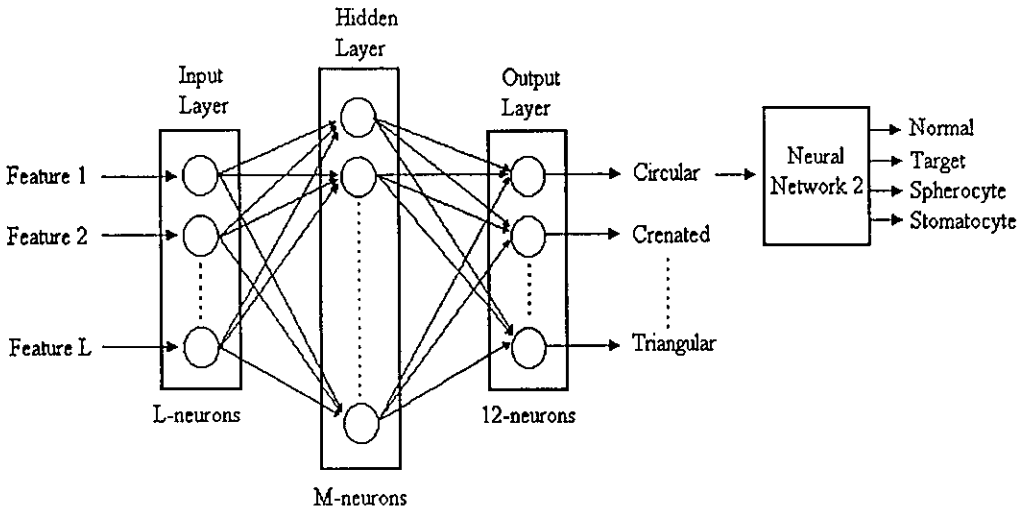

Fig. 7. Neural network architecture to classify red-blood cells

The back-propagation learning algorithm is a general delta rule that controls the weighting factor by the following equation.

$$W(new)_{ij} = W(old)_{ij} + \alpha\delta_j a_i \tag{5}$$

where i,j : a neuron in the hidden and output layer, respectively,
$W(new)_{ij}$: modified weight between neuron i and neuron j,
$W(old)_{ij}$: previous weight between neuron i and neuron j,
$e_j = t_j - a_j$: neuron error in output layer,
$e_j = \sum_k W_{jk}\delta_k$: neuron error in hidden layer,
$\delta_j = a_i(1 - a_j)e_j$: delta of neuron j,
α : learning rate,
a_i: activation value of neuron i,
a_j: activation value of neuron j,
e_j: error of neuron j,
t_j: value of target pattern if neuron j is in output layer,
W_{jk}: weight of neuron k in previous layer if neuron j is in the hidden layer,
δ_k: delta of neuron k in previous layer if neuron j is in the hidden layer.

We use an adaptive learning algorithm to reduce the learning time of the neural network and to find the local minima. Let $W_{ij}(old)$ be the current weight

ınd $W_{ij}(older)$ be the previous weight. The current momentum is the difference ›etween the current weight and the previous weight. Therefore, the general delta ·ule can be modified as

$$W(new)_{ij} = W(old)_{ij} + \alpha\delta_j a_i + \beta\Delta W_{ij}(old) \quad (6)$$

.vhere β is a constant that controls the momentum.

Table 1. Parameter values for neural networks

Classifier	Parameter						
	Slope of activation function	Learning constant	Nodes for input layer	Hidden layer	Nodes for hidden layer	Nodes for output layer	Momentum constant
NN 1	0.1	0.5	38	2	125	12	0.9
NN 2	0.1	0.5	38	1	120	4	0.9
NN 3	0.1	0.5	52	1	80	5	0.9

3 Experimental Results

In our experiment, we have used Wright dyed blood images collected from two hundred patients in the hospital. In order to train the classifier, we use 680 test cells for fifteen classes of red-blood cells, and 70 of monocyte, 50 of basophil, 120 of neutrophil, 50 of esinophil, and 120 of lymphocyte for five classes of white-blood cells. The data set is verified by human expert. We select the leave-one-out method for the test and apply PCA to reduce the feature dimension. The original feature dimension of 76 has been reduced to 38 in the first recognition step, 67 in the second one for the red-blood cells. The initial 60 dimensional features for white-blood cells are reduced to 52 dimension.

We have compared our classifier to other two classifiers, K-NN and LVQ-3 for classifying red-blood cells. Figure 8 shows recognition rates for red-blood cells in the first and the second steps, respectively. Figure 9 shows the improved recognition rates acquired with the reduced features after applying PCA. MLP in Figure 8 and Figure 9 indicates our classifier based on the multiplayer perceptron.

After classification, the result is compared with that of human expert. Our experimental results show that we can obtain improved recognition rates using features of reduced dimension. However, the recognition rate is low in the first step, since it is difficult to distinguish burr cells from crenated cells with nearly the same contour shape. This problem can be improved by more precise contour extraction. Table 2 and Table 3 list the average recognition rates with the original features and the reduced features, respectively.

Table 4 presents the final recognition result of white-blood cells by a confusion matrix with the reduced features. As we can observe in Table 4, most recognition errors are between monocyte and lymphocyte and between neutrophil and esinophil, since they have the same characteristics in the shape, the size and the color of the nucleus and cytoplasm. Moreover, it is very difficult even for a human expert to distinguish the monocyte from the abnormal lymphocyte, because they have the same characteristics in terms of the size, color and ratio of neucleus and cyteoplasm.

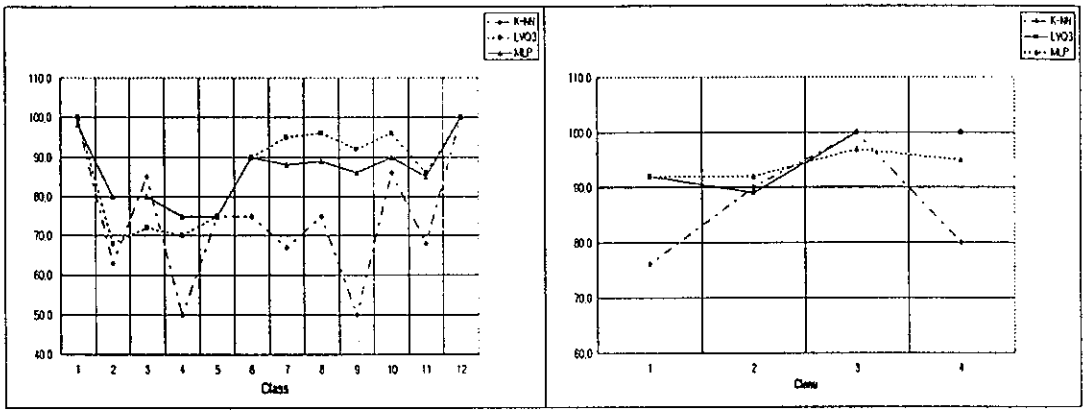

(a) First step (b) Second step

Fig. 8. Recognition rate (%) of red-blood cells

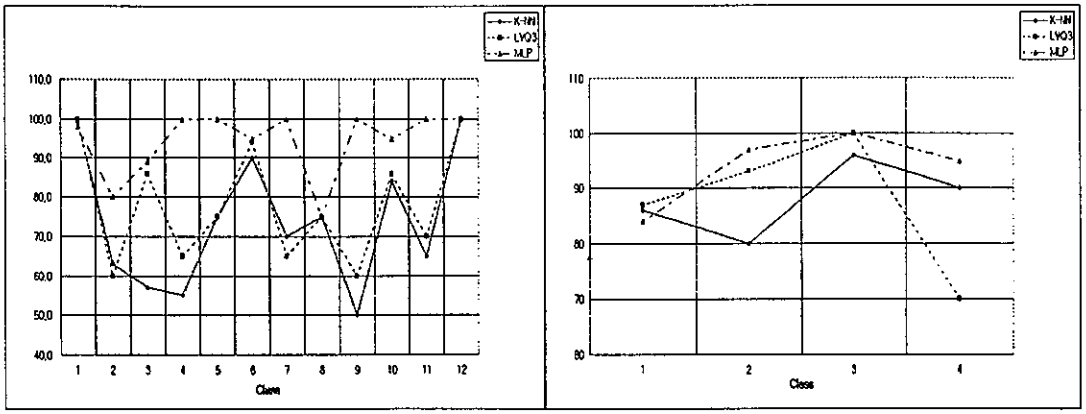

(a) First step (b) Second step

Fig. 9. Recognition rate (%) after PCA

Table 2. Average recognition rate (%) before PCA

Recognition Step	Classifier		
	K-NN	LVQ-3	MLP
Second Step (12 Classes)	75	87	87
Second Step (4 Classes)	90	91	94

Table 3. Average recognition rate (%) after PCA

Recognition Step	Classifier		
	K-NN	LVQ-3	MLP
Second Step (12 Classes)	73	78	87
Second Step (4 Classes)	88	87	94

Table 4. Confusion matrix for white-blood cells

Input \ Output	Monocyte	Basophil	Neutrophil	Esinophil	Lymphocyte
Monocyte	55	0	2	0	13
Basophil	0	38	2	10	0
Neutrophil	11	0	97	8	4
Esinophil	0	2	6	42	0
Lymphocyte	8	0	4	0	98

4 Conclusions

In this paper, we have proposed a new scheme to recognize and classify red-blood and white-blood cells in the human peripheral blood image. We have also described a classification model based on the neural network. We classify red-blood cells in two steps using inner edges and contour information, and white-blood cells using various features of the nucleus and cytoplasm. We have proposed a new algorithm to segment the nucleus and cytoplasm of white-blood cells. In addition, we show that complexity of the neural network can be reduced and a more efficient system can be constructed by applying PCA to features extracted from cells. The recognition rate for red-blood and white-blood cells is 91% and 81% on average, respectively.

Acknowledgment

This work was supported in part by the Korea Science and Engineering Foundation (KOSEF) through the Ultra-Fast Fiber-Optic Networks (UFON) Research Center at Kwangju Institute of Science and Technology (K-JIST), and in part by the Ministry of Education (MOE) through the Brain Korea 21 (BK21) project.

References

1. Comaniciu, D., Meer, P., Foran, D.: Image Guided Decision Support System for Pathology, Machine Vision and Applications, Vol. 11, No. 4 (2000) 213-224
2. Freeman, J.A., Skapura, D.M., Neural Networks: Algorithms, Applications and Programming, Techniques. Addision-Wesley Publishing (1991)
3. Huang, L.K, Wang, M. J.: Image Thresholding by Minimizing the Measures of Fuzziness, Pattern Recognition, Vol.28 (1995) 1:41-51
4. Jang, Y.H.: Optimal Neural Network Classifier for Chromosome Karyotype Classification, KIEE Journal, Vol.46, No.7, Jul. (1997) 1129-1134
5. Korea Medical Publisher: Illustrated Hematology Book. Korea Publishing (1995)
6. Majman, L., Schmitt, M.: Geodesic Saliency of Watershed Contours and Hierarchical Segmentation, IEEE Trans. on Pattern Analysis and Machine Intelligence, Vol.18, No.12 (1996) 1163-1173
7. Mehtre, B.M., Kankanhalli, M.S., Lee, W. F.: Shape Measures For Content Based Image Retrieval: A Comparison, Technical Report 95-195-0, Institute of Systems Science, National University of Singapore (1995)
8. Moga, N.A., Gabbouj, M. : Parallel Image Component Labeling with Watershed Transformation, IEEE Trans. on Pattern Analysis and Machine Intelligence, Vol.19, No.5 (1997) 441-450
9. Nagata, H., Mizushima, H.: World Wide Microscope: New Concept of Internet Telepathology Microscope and Implementation of the Prototype, MEDIINFO 98 (1998) 286-289
10. Perona, P., Malik, M.: Scale-Space and Edge Detection using Anisotropic Diffusion, IEEE Trans. on Pattern analysis and machine intelligence, Vol.12, No.7 (1990) 629-639
11. Rauber, T.W.: Two-Dimensional Shape Description, Technical Report Gruninova-RT-10-94, Universidade Nova de Lisboa, Lisboa, Portugal (1994)
12. Seker, S., Bagriyanik, M., Gabgriyanik, F.G.: An Application of Shannon's Entropy for Neural Architecture, Proc. of the 15th IASTED, Innsbruck (1997) 33-36
13. Stewart, B.K., Langer, S.G.: Medical Image Databases and Informatics, IEEE International Conf. on image processing, Oct. 4-7, Chicago, Illinois (1998) 29-33